The ROYAL COLLEGE of
OPHTHALMOLOGISTS

ARTICLE

Widefield topographical analysis of the retinal perfusion and neuroretinal thickness in healthy eyes: a pilot study

Enrico Borrelli [1] · Lisa Toto [1] · Pasquale Viggiano[1] · Federica Evangelista[1] · Michele Palmieri[1] · Rodolfo Mastropasqua[2]

Abstract

Purpose In this pilot study we reported variation of superficial (SCP) and deep (DCP) capillary plexuses flow in macular and near/mid periphery regions in healthy subjects using widefield swept source-optical coherence tomography angiography (SS-OCTA).

Methods In this prospective, cross-sectional study, enroled subjects were imaged with an SS-OCTA system (PLEX Elite 9000, Carl Zeiss Meditec Inc., Dublin, CA, USA). OCTA scans were taken in primary and extremes of gaze and a montage was automatically created. Quantitative analysis was performed in the macular and peripheral regions. In addition, SCP and DCP variables were further investigated in distinct fields within these three different regions.

Results Fifty-five young healthy subjects (55 eyes) were enroled. The retinal periphery displayed a higher SCP perfusion density ($39.6 \pm 1.7\%$ and $40.7 \pm 1.4\%$, $P < 0.0001$) and SCP vessel diameter index (3.5 ± 0.2 and 3.6 ± 0.2, $P < 0.0001$), in comparison with the macular region. At the DCP level, the retinal periphery was characterized by a lower perfusion density ($41.6 \pm 3.7\%$ and $37.9 \pm 2.9\%$, $P < 0.0001$) and vessel length density ($14.6 \pm 6.0\%$ and $9.9 \pm 2.6\%$, $P < 0.0001$). In the analysis investigating the DCP in the retinal periphery, the temporal sector was characterized by a reduction in perfusion density, vessel length density, and vessel diameter index. In univariate analysis, the retinal thickness was found to have a significant direct relationship with DCP perfusion density ($P < 0.0001$), but not with SCP perfusion density ($P = 0.712$).

Conclusions We report quantitative mapping of the SCP and DCP in healthy individuals. The DCP perfusion appears to have a wide topographical variation, which is strictly dependent on the retinal thickness.

Introduction

The retinal vascularization is composed of a highly anastomosed network of capillaries which are responsible of nourishing the neuroretina. Based on recent optical coherence tomography angiography (OCTA) studies in adults, vessels located in the retinal nerve fibre and ganglion cell layers constitute the superficial retinal capillary plexus (SCP), while the middle capillary plexus and the deep retinal capillary plexus (DCP) are located at the inner and outer borders of the inner nuclear layer, respectively [1–4].

Of note, these plexuses are interconnected through small vessels in vertical course [5].

OCTA, still a rapidly evolving technology, has proven to be a valuable tool for the depth-resolved evaluation of the retinal circulation in several ocular and systemic disorders, including diabetes, age-related macular degeneration, and myopia [6]. However, one of the most relevant limitations of these studies using OCTA was the scanning region limited to the macula.

The recent introduction of high-speed swept source OCTA devices is expected to significantly expand the evaluation of the retinal capillary network. These devices with a higher speed system allow for acquiring a larger field of view [7, 8]. A wider region of OCTA assessment might provide more details about retinal and vascular disorders not limited to the macula and help in determining new imaging biomarkers of disease.

In this pilot study we sought to report normal measurements of the SCP and DCP in healthy young individuals

✉ Enrico Borrelli
borrelli.enrico@yahoo.com

1   Ophthalmology Clinic, Department of Medicine and Science of Ageing, University G. D'Annunzio Chieti-Pescara, Chieti, Italy

2   Bristol Eye Hospital, Bristol, UK

using widefield SS-OCTA analysis. In details, these measurements were determined in different retinal regions in order to provide a topographical analysis of the SCP and DCP perfusion. Establishing healthy OCTA reference parameters of the retinal vascularization is essential for proper interpretation of pathological values.

Methods

Study participants

In this prospective observational cross-sectional study, healthy subjects between 18 and 40 years of age were enroled at the ophthalmology clinic of University G. d'Annunzio, Chieti-Pescara, Italy. The study was approved by the Institutional Review Board (IRB) and adhered to the tenets of the Declaration of Helsinki. An IRB approved informed consent was obtained from all subjects.

All subjects enroled were imaged with the PLEX Elite 9000 device (Carl Zeiss Meditec Inc., Dublin, CA, USA) between April 2018 and August 2018. Moreover, all subjects received a complete ophthalmologic examination, which included the measurement of best-corrected visual acuity, intraocular pressure, and dilated ophthalmoscopy. Exclusion criteria were (i) evidence or history of ocular diseases; (ii) evidence or history of systemic disorders, including diabetes and systemic hypertension; (iii) history of previous ocular surgery; (iv) ocular axial length greater than 26 mm.

Imaging

Subjects underwent OCTA imaging using the PLEX Elite 9000 device (Carl Zeiss Meditec Inc., Dublin, CA, USA) which uses a swept laser source with a central wavelength of 1050 nm (1000–1100 nm full bandwidth) and operates at 100,000 A-scans per second. This instrument employs a full-width at half-maximum (FWHM) axial resolution of ~5 μm in tissue, and a lateral resolution at the retinal surface estimated at ~14 μm.

For each eye, five 12×12-mm OCTA volume scans were acquired. These scans were acquired in five different subject's gazes (central, nasal inferior, nasal superior, temporal inferior, and temporal superior) by moving the internal fixation light. For each eye we thus obtained five OCTA scans from five distinct and partially overlapping retinal regions. Poor quality images (signal strength index (SSI) < 8) with either significant motion artefact or incorrect segmentation were excluded and repeated. Finally, the built-in software included in the device automatically combined these five scans in a final montage image. After realizing the montage, images with significant artefacts in the tested

regions were not included in the analysis. In order to account for the intra-subject inter-eye correlation, we did include only one eye for each subject. In detail, for each subject, the eye with the OCTA image with the highest SSI was included. In those cases, characterized by the same SSI for both eyes, the right eye was finally included in the analysis.

Image processing

The main outcome measures were: (i) SCP perfusion and vessel densities; (ii) DCP perfusion and vessel densities; and (iii) SCP and DCP vessel diameter index.

In order to quantify these variables, a slightly modified previously reported semi-automated algorithm was employed [9–11]. In brief, for each eye, en face OCTA images segmented at the SCP and DCP levels were imported into ImageJ software version 1.50 (National Institutes of Health, Bethesda, MD; available at http://rsb.info.nih.gov/ij/index.html) and, consequently were processed with a "top-hat" filter. Each image was duplicated and two different binarizarion methods were then performed on the two resultant images: (i) one image was first processed by a "hessian" filter, followed by global thresholding using the "Huang's fuzzy" method; (ii) the other (duplicate) image was binarized using the "median local" thresholding. Finally, the two obtained images were combined.

The perfusion density (PD) was thus calculated as a unitless proportion of the number of pixels over the threshold divided by the total number of pixels in the analysed area. Successively, the SCP and DCP images obtained after binarization were skeletonized and these images were employed to measure the vessel length density (VLD) [10–12]. In order to measure the average vessel calibre, we calculated the vessel diameter index (VDI) by dividing the area in the binarized image by that in the skeletonized image [10, 11]. The DCP directly beneath major superficial retinal vessels was excluded from analysis to eliminate potentially confounding shadow or projection artefacts, as previously shown [10, 11].

The quantitative analysis was thus performed in two different regions: (i) *macular region*, which was defined as a circular annulus around the fovea with diameter of 5.5 mm and excluding the foveal avascular zone, and (ii) *periphery region* which was assessed in three circles tangential to the macula and with diameters of 4.5 mm (Figs. 1 and 2) [13]. The latter choice was made to investigate the SCP and the DCP in the near and mid periphery (1.5-mm-wide annulus around the macula and 3.0-mm-wide annulus around the near periphery, respectively) and consequently to exclude the far periphery from the analysis (see "Discussion").
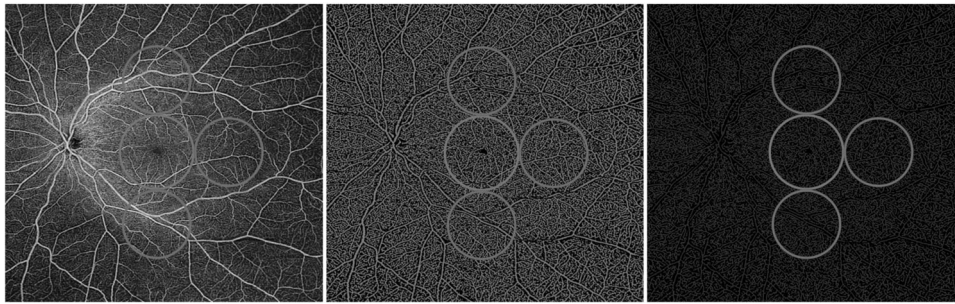
Fig. 1 Representation of the widefield OCTA assessment of the superficial capillary plexus. (Left image) The superficial capillary plexus (SCP) was investigated in two different regions: (i) macular region (red circle) with a diameter of 5.5 mm; and (ii) periphery region which was assessed in three circles tangential to the macula (blue circles) and with diameters of 4.5 mm. The SCP binarized (middle) and skeletonized (right) images were analysed to investigate the SCP perfusion and vessel length density, respectively.
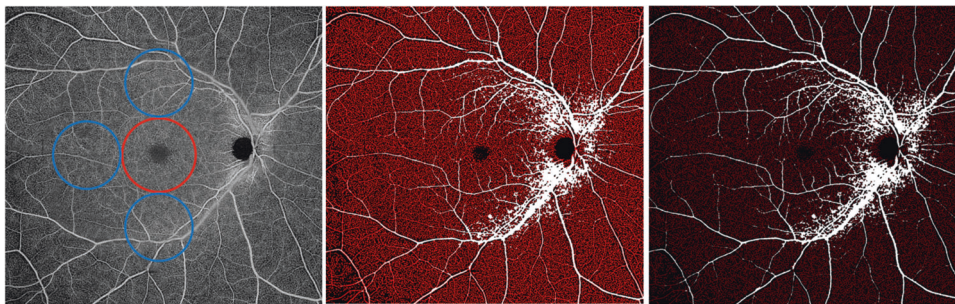
Fig. 2 Representation of the widefield OCTA assessment of the deep capillary plexus. (Left image) The deep capillary plexus (DCP) was investigated in two different regions: (i) macular region (red circle) with a diameter of 5.5 mm; and (ii) periphery region which was assessed in three circles tangential to the macula (blue circles) and with diameters of 4.5 mm. The DCP binarized (middle) and skeletonized (right) images were analysed to investigate the DCP perfusion and vessel length density, respectively. The superficial capillary plexus' big retinal vessels were identified and masked in the DCP image (white vessels), in order to avoid shadowing and projection artefacts from confounding the analysis of this slab.

Furthermore, the analysis of the periphery was further performed in different sub-fields, since this region was split into the superior, temporal, and inferior areas.

In order to assess reproducibility of our measurements, 15 healthy subjects underwent second OCTA measurements in a different day.

Statistical analysis

All quantitative variables were reported as mean and standard deviation (SD) in the "Results" section and in the Tables.

To detect departures from normality distribution, Shapiro–Wilk's test was performed for all variables, which demonstrated a normal distribution. Parametric tests were carried out to assess quantitative differences among variables. The analysis of variance was used to assess the reproducibility between the two measurements.

Statistical calculations were performed using Statistical Package for Social Sciences (version 20.0, SPSS Inc., Chicago, IL, USA). The chosen level of statistical significance was $p < 0.05$.

Results

Characteristics of subjects included in the analysis

Of the 55 eyes (55 individuals) that were initially enroled, 52 eyes met the required image quality criteria and were used in the analysis. Mean ± SD age was 25.4 ± 5.3 years [median: 24.5 years; range: 20.0–40.0 years]. Mean ± SD axial length was 23.2 ± 1.0 mm [median: 23.9 mm; range: 21.8–25.9 mm].

Widefield OCTA and OCT analysis of the retinal vessels

The difference between the two measurements was not statistically significant in all the analysed regions ($p = 1.0$ for the SCP macular region, $p = 0.65$ for the SCP peripheral region, $p = 0.91$ for the DCP macular region, and $p = 0.11$ for the DCP peripheral region), indicating an overall good reproducibility.

The retinal periphery displayed a higher SCP PD (39.6 ± 1.7% and 40.7 ± 1.4%, $P < 0.0001$) and SCP VDI (3.5 ± 0.2 and 3.6 ± 0.2, $P < 0.0001$), in comparison with the macular

Table 1 OCTA tested variables in the analysed regions.

	Macula	Periphery	P value
OCTA			
SCP perfusion density (%)	39.6 ± 1.7	40.7 ± 1.4	<0.0001
SCP vessel length density (%)	11.1 ± 0.6	11.2 ± 0.6	0.319
SCP vessel diameter index	3.5 ± 0.2	3.6 ± 0.2	<0.0001
DCP perfusion density (%)	41.6 ± 3.7	37.9 ± 2.9	<0.0001
DCP vessel length density (%)	14.6 ± 6.0	9.9 ± 2.6	<0.0001
DCP vessel diameter index	3.6 ± 0.2	3.5 ± 0.9	0.674
OCT			
Retinal thickness (μm)	259.5 ± 16.9	214.2 ± 13.2	<0.0001

Data are presented as mean ± SD (standard deviation).

OCTA optical coherence tomography angiography, *OCT* optical coherence tomography, *SCP* superficial capillary plexus, *DCP* deep capillary plexus.

Table 2 OCTA tested variables in the periphery.

	Superior	Temporal	Inferior
OCTA			
SCP perfusion density (%)	40.6 ± 1.8	40.5 ± 1.4	41.0 ± 1.5
		>0.050[a]	>0.050[a]
	–		>0.050[b]
SCP vessel length density (%)	11.2 ± 0.6	11.3 ± 0.6	11.2 ± 0.6
		>0.050[a]	>0.050[a]
	–		>0.050[b]
SCP vessel diameter index	3.6 ± 0.2	3.6 ± 0.2	3.7 ± 0.2
		0.424[a]	<0.0001[a]
	–		<0.0001[b]
DCP perfusion density (%)	45.5 ± 7.4	41.3 ± 1.5	44.8 ± 7.2
		<0.0001[a]	0.108[a]
	–		<0.0001[b]
DCP vessel length density (%)	22.5 ± 11.9	13.3 ± 2.3	21.7 ± 11.2
		<0.0001[a]	0.645[a]
	–		<0.0001[b]
DCP vessel diameter index	3.7 ± 0.2	3.6 ± 0.5	3.7 ± 0.2
		0.043[a]	0.607[a]
	–		0.001[b]
OCT			
Retinal thickness (μm)	259.5 ± 16.9	214.2 ± 13.2	214.2 ± 13.2
		0.043[a]	0.607[a]
	–		0.001[b]

Data are presented as mean ± SD (standard deviation).

OCTA optical coherence tomography angiography, *OCT* optical coherence tomography, *SCP* superficial capillary plexus, *DCP* deep capillary plexus.

[a]Comparison versus "Superior region".

[b]Comparison versus "Temporal region".

region. On contrary, no differences were found in terms of VLD between these two regions ($P = 0.319$) (Table 1).

At the DCP level, the retinal periphery was characterized by a lower PD ($41.6 ± 3.7\%$ and $37.9 ± 2.9\%$, $P < 0.0001$) and VLD ($14.6 ± 6.0\%$ and $9.9 ± 2.6\%$, $P < 0.0001$). The VDI was $3.6 ± 0.2$ in the retinal periphery and $3.5 ± 0.9$ in the macular region ($P = 0.674$) (Table 1).

The retinal thickness was $259.5 ± 16.9$ μm in the macular region and $212.0 ± 13.1$ μm in the peripheral region ($P < 0.0001$) (Table 1).

In the analysis investigating the DCP in the retinal periphery, the temporal sector was characterized by a lower PD ($P < 0.0001$ in the comparison with both the superior and inferior regions), reduced VLD ($P < 0.0001$ vs the superior and inferior regions), and contracted VDI ($P = 0.043$ vs the superior sector and $P = 0.001$ vs the inferior sector) (Table 2). The SCP perfusion and vessel length densities did not display differences among the retinal periphery regions. The SCP VDI was increased in the inferior sector ($P < 0.0001$ in the comparison with both the superior and temporal regions) (Table 2).

The retinal thickness was $195.3 ± 14.2$ μm in the temporal field ($P < 0.0001$ in the comparison with both superior and inferior fields), $220.5 ± 14.9$ μm in the superior field ($P = 1.0$ vs the inferior field), and $219.5 ± 14.7$ μm in the inferior field (Table 2).

In univariate analysis, the retinal thickness was found to have a significant direct relationship with DCP PD ($P < 0.0001$), but not with SCP PD ($P = 0.712$). Likewise, the retinal thickness had a significant direct relationship with DCP VLD ($P < 0.0001$), but not with SCP VLD ($P = 0.670$).

Discussion

In this cross-sectional study we report quantitative mapping of the retinal vessels in healthy eyes using widefield

SS-OCTA. We found regional differences in the retinal perfusion which should be considered as OCTA-based parameters are increasingly used for the diagnosis of retinal vascular disorders. Importantly, these differences were mainly limited to the DCP. In details, our results illustrated that the macula displays an increased number of capillaries in comparison with the near/mid periphery. Furthermore, a topographical sub-analysis within the near/mid periphery revealed that the DCP does not exhibit a uniform vascular density and that these differences are correlated to the retinal thickness. Importantly, in the assessment of the retinal vessels in the retinal periphery, we excluded the far periphery from the evaluation. This assessment is indeed still limited by significant shadowing artefacts, given that the very large depth of field commonly results in the subject's eyelashes to appear in the image. Thus, we felt the safer strategy was to look just at the near/mid periphery.

While the introduction of OCTA has significantly expanded the evaluation of the retinal capillaries, previous notable studies investigating these vessels were limited to assess the macular region. The SCP and DCP perfusion in

this field was demonstrated to be inversely correlated with age and disease (e.g. myopia, hypertension, and age-related macular degeneration) [6, 14–16]. Using widefield SS-OCTA imaging, we add to the literature by reporting both perfusion and vessel length densities in the retinal periphery. While PD is investigated on binarized images and is thus based on the perfused vascular area, VLD is assessed on skeletonized images which create a map with vessels of 1-pixel width. Since in the VLD assessment thicker and thinner vessels have the same weight on the final density, the vessel length and perfusion densities are thus dependent on a one-dimensional (only length) and two-dimensional (length and width) quantification of the retinal vasculature, respectively [10–12]. The estimation and discrimination of these two parameters may allow for a better understanding of the retinal vessels' physiological and pathological changes, given that differences may be secondary to either a contraction in retinal vessel calibre or a decrease in branching patterns, as previously suggested [10, 11].

We demonstrated that both SCP and DCP significantly differ between macular and peripheral regions. In details, the SCP was characterized by an increased PD in the peripheral region. On contrary, the SCP VLD did not display significant differences between these two regions. This apparent discrepancy between increased PD and unchanged VLD is justified by an increased vessel diameter in the peripheral region. The latter finding is in agreement with previous histopathological studies showing that the major temporal vascular arcades are located in the near/mid periphery [17]. Notably, the DCP displayed a significant reduction in perfusion and vessel length densities in the peripheral region, along with an unvaried vessel diameter. Taken together, these results may suggest that the retinal capillaries located at the DCP level become progressively lower toward the periphery, even maintaining the same vessel diameter.

In our adult healthy cohort, we also assessed topographical differences in SCP and DCP vasculature within the peripheral region. One of the most notable observations from our study was that the DCP PD was significantly lower in the temporal field. Importantly, this reduction in PD is ascribable to both a lower number of vessels and a decrease in their diameter.

Using widefield OCTA, Jia et al. [18] examined the radial peripapillary capillary plexus flow characteristics in ten eyes of ten healthy subjects and illustrated an association between perfusion in this vascular network and nerve fibre layer thickness. Similarly, the present study highlights the distinctive relationship between neuroretinal thickness and DCP PD—considering DCP PD as dependent variable, we observed a direct relationship between these two variables. In addition, the retinal thickness displayed a similar topographical variability to that demonstrated for the DCP

perfusion and vessel length densities: the neuroretinal thickness is highest in the macular region and lowest in the temporal peripheral field. Our results highlight that the morphology of the retinal capillary networks is coupled with the metabolic demands of the neuroretina, which requires efficient delivery of oxygen and metabolites. Accordingly, the macula, which includes a high density of rod and ganglion cells and is considered one of the highest energy demanding tissues of the human body [3, 19], displayed the highest DCP vascular density.

Notably, we demonstrated that the retinal thickness was strongly associated with the DCP perfusion, but not with the SCP perfusion. Previous studies in animal models demonstrated that the dominant oxygen consumers of the neuroretina are located in the plexiform layers [20–24]. Moreover, the retinal capillaries located deeper in the retina are thought to originate from the SCP, this process guided by the hypoxia of glia and neurons located deeper in the retina and producing vascular endothelial growth factor [25]. Given this, we might thus speculate that retinal depth may drive the development of retinal vessels in the DCP, whose density is thus dependent on the retinal thickness.

Our findings also have implications in the clinical use of widefield OCTA to evaluate retinal vascular disorders. In areas where the DCP perfusion is high, minor loss of capillaries may not be easily detected. Therefore, future studies employing widefield OCTA may clarify whether the peripheral regions may be preferred to detect early vascular changes in retinal vascular disorders.

Our study has limitations including the cross-sectional nature of the study. A prospective longitudinal evaluation of the retinal vessels in healthy eyes may shed further light on the causal role of the retinal vasculature in the development of retinal vascular disorders. For example, it would be interesting to know whether these regional differences in DCP perfusion may represent a risk factor for the development of certain disorders. Furthermore, the 12×12-mm scan has limited resolution and we are not able to exclude that this may have impacted our results. However, widefield OCTA imaging is still a technology in evolution, and the optimal technological approach has yet to be reached. Furthermore, while we excluded the far peripheral regions from the analysis in order to avoid eyelashes artefacts from confounding the quantitative assessment [26, 27], we are not able to exclude that these artefacts may have impacted, at least in part, also the investigation of the inferior and superior near/mid periphery regions. One would expect, however, that with the presence of shadowing artefacts there would be an artefactitiously lower perfusion of the superior and inferior regions. In contrast, in our study, we observed a higher perfusion in these regions. This difference with the temporal region may have actually been an underestimate. Moreover, our study was aimed at describing

SCP and DCP vessels in healthy young subjects (mean ± SD age of 25.2 ± 5.1 years) and we thus included healthy eyes with narrow range of axial length (mean ± SD: 23.9 ± 1.1 mm), therefore, we were unable to comment upon the effect of these two variables (age and axial length) on widefield SCP and DCP vascular densities. Finally, examinations were performed at variable times during the day. Although OCTA is known to be characterized by a high reproducibility [28, 29], we are not able to exclude that this variability may have impacted on our results.

In summary, in this pilot widefield SS-OCTA study of the retinal vessels, we observed that healthy eyes have topographical variability in SCP and DCP flow. Future studies with extended longitudinal follow-up and further analysis of age and axial length on retinal vasculature may provide additional substantive information. These results should be considered in OCTA-based studies of affected eyes.

Summary

What was known before

- Quantitative analysis in macular region.

What this study adds

- Quantitative analysis in macular and near/mid periphery regions.

Compliance with ethical standards

References

1. Savastano MC, Lumbroso B, Rispoli M. In vivo characterization of retinal vascularization morphology using optical coherence tomography angiography. Retina. 2015. https://doi.org/10.1097/IAE.0000000000000635.
2. Park JJ, Soetikno BT, Fawzi AA. Characterization of the middle capillary plexus using optical coherence tomography angiography in healthy and diabetic eyes. Retina. 2016;36:2039–50. https://doi.org/10.1097/IAE.0000000000001077.
3. Yu D-Y, Yu PK, Cringle SJ, Kang MH, Su E-N. Functional and morphological characteristics of the retinal and choroidal vasculature. Prog Retin Eye Res. 2014;40:53–93. https://doi.org/10.1016/j.preteyeres.2014.02.001.
4. Borrelli E, Sadda SR, Uji A, Querques G. Pearls and pitfalls of optical coherence tomography angiography imaging: a review. Ophthalmol Ther. 2019. https://doi.org/10.1007/s40123-019-0178-6.
5. Nesper PL, Fawzi AA. Human parafoveal capillary vascular anatomy and connectivity revealed by optical coherence tomography angiography. Investig Ophthalmol Vis Sci. 2018. https://doi.org/10.1167/iovs.18-24710.
6. Spaide R, Fujimoto JG, Waheed NK, Sadda SR, Staurenghi G. Optical coherence tomography angiography. Prog Retin Eye Res. 2017. https://doi.org/10.1016/j.preteyeres.2017.11.003.
7. Liu G, Yang J, Wang J, et al. Extended axial imaging range, widefield swept source optical coherence tomography angiography. J Biophotonics. 2017;10:1464–72. https://doi.org/10.1002/jbio.201600325.
8. Sawada O, Ichiyama Y, Obata S, et al. Comparison between wide-angle OCT angiography and ultra-wide field fluorescein angiography for detecting non-perfusion areas and retinal neovascularization in eyes with diabetic retinopathy. Graefe's Arch Clin Exp Ophthalmol. 2018;256:1275–80. https://doi.org/10.1007/s00417-018-3992-y.
9. Uji A, Balasubramanian S, Lei J, Baghdasaryan E, Al-Sheikh M, Sadda SR. Impact of multiple en face image averaging on quantitative assessment from optical coherence tomography angiography images. Ophthalmology. 2017. https://doi.org/10.1016/j.ophtha.2017.02.006.
10. Borrelli E, Lonngi M, Balasubramanian S, et al. Macular microvascular networks in healthy pediatric subjects. Retina. 2018. https://doi.org/10.1097/IAE.0000000000002123.
11. Borrelli E, Balasubramanian S, Triolo G, Barboni P, Sadda SR, Sadun AA. Topographic macular microvascular changes and correlation with visual loss in chronic leber hereditary optic neuropathy. Am J Ophthalmol. 2018;192:217–28. https://doi.org/10.1016/j.ajo.2018.05.029.
12. Durbin MK, An L, Shemonski ND. et al. Quantification of retinal microvascular density in optical coherence tomographic angiography images in diabetic retinopathy. JAMA Ophthalmol. 2017;135:370.
13. Forrester JV, Dick AD, McMenamin PG, Roberts F, Pearlman E. The eye: basic sciences in practice. Elsevier. 2008. p. 568. https://doi.org/10.1038/nrg1202.J.
14. Toto L, Borrelli E, Di Antonio L, Carpineto P, Mastropasqua R. Retinal vascular plexuses' changes in dry age-related by means of optical coherence. Retina. https://doi.org/10.1097/IAE.0000000000000962.
15. Iafe NA, Phasukkijwatana N, Chen X, Sarraf D. Retinal capillary density and foveal avascular zone area are age-dependent: quantitative analysis using optical coherence tomography angiography. Investig Opthalmology Vis Sci. 2016;57:5780. https://doi.org/10.1167/iovs.16-20045.
16. Al-Sheikh M, Phasukkijwatana N, Dolz-Marco R, et al. Quantitative OCT angiography of the retinal microvasculature and the choriocapillaris in myopic eyes. Investig Ophthalmol Vis Sci. 2017;58:2063–9. https://doi.org/10.1167/iovs.16-21289.
17. Schachat AP, Sadda SR, Hinton DR, Wilkinson CP, Wiedemann P, editors. Ryan's. Retina. 6th ed. New York: Elsevier; 2018.
18. Jia Y, Simonett JM, Wang J, et al. Wide-field OCT angiography investigation of the relationship between radial peripapillary capillary plexus density and nerve fiber layer thickness. Investig Ophthalmol Vis Sci. 2017. https://doi.org/10.1167/iovs.17-22593.

19. Provis JM, Penfold PL, Cornish EE, Sandercoe TM, Madigan MC. Anatomy and development of the macula: specialisation and the vulnerability to macular degeneration. Clin Exp Optom. 2005;88:269–81. http://www.ncbi.nlm.nih.gov/pubmed/16255686.

20. Yu DY, Cringle SJ, Su EN. Intraretinal oxygen distribution in the monkey retina and the response to systemic hyperoxia. Investig Ophthalmol Vis Sci. 2005. https://doi.org/10.1167/iovs.05-0694.

21. Yu DY, Cringle SJ, Yu PK, Su EN. Intraretinal oxygen distribution and consumption during retinal artery occlusion and graded hyperoxic ventilation in the rat. Investig Ophthalmol Vis Sci. 2007. https://doi.org/10.1167/iovs.06-1197.

22. Cringle SJ, Yu DY, Yu PK, Su EN. Intraretinal oxygen consumption in the rat in vivo. Investig Ophthalmol Vis Sci. 2002.

23. Yu DY, Cringle SJ, Alder V, Su EN. Intraretinal oxygen distribution in the rat with graded systemic hyperoxia and hypercapnia. Investig Ophthalmol Vis Sci. 1999.

24. Yu DY, Cringle SJ, Alder VA, Su EN. Intraretinal oxygen distribution in rats as a function of systemic blood pressure. Am J Physiol. 1994. https://doi.org/10.1152/ajpheart.1994.267.6.H2498.

25. Provis JM. Development of the primate retinal vasculature. Prog Retin Eye Res. 2001. https://doi.org/10.1016/S1350-9462(01)00012-X.

26. Borrelli E, Viggiano P, Evangelista F, Toto L, Mastropasqua R. Eyelashes artifact in ultra-widefield optical coherence tomography angiography. Ophthalmic Surg Lasers Imaging Retin. 2019.

27. Borrelli E, Uji A, Toto L, Viggiano P, Evangelista F, Mastropasqua R. In vivo mapping of the choriocapillaris in healthy eyes: a widefield swept source optical coherence tomography angiography study. Ophthalmol Retina. 2019;3:979–84. https://doi.org/10.1016/j.oret.2019.05.026.

28. Lei J, Durbin MK, Shi Y, et al. Repeatability and reproducibility of superficial macular retinal vessel density measurements using optical coherence tomography angiography en face images. JAMA Ophthalmol. 2017;135:1092–8. https://doi.org/10.1001/jamaophthalmol.2017.3431.

29. Al-Sheikh M, Tepelus TC, Nazikyan T, Sadda SVR. Repeatability of automated vessel density measurements using optical coherence tomography angiography. Br J Ophthalmol. 2017. https://doi.org/10.1136/bjophthalmol-2016-308764.